



τ -lepton Studies within Belle II Experiment

Yurii Kvasiuk, Taras Shevchenko National University of Kyiv, Ukraine

Supervisor: Dr. Armine Rostomyan

September 7, 2018

Abstract

The cross section of the tau-pair production is compatible to the one of B mesons at the energies of B-factories. The upcoming Belle II experiment will collect a huge amount of data starting next year. This work is dedicated to optimization of τ -pair selection using the Monte Carlo simulations. The invariant mass of the 3-prong tau-decays from Phase 2 data of Belle II is obtained and compared to Monte Carlo simulations.

Contents

- 1 Introduction** **3**
- 2 Tau Properties Overview** **4**
- 3 Event Selection** **6**
- 4 Analysis** **7**
 - 4.1 Distribution Shape Overview 7
 - 4.2 Figure of Merit 8
- 5 Conclusions** **11**
- 6 Appendix** **13**

1 Introduction

Studying properties of leptons and other elementary particles could be a probing tool for Standard Model or a tool for finding new phenomena that give the possibility for new physics to rise. Studies of decays of τ -leptons, the heaviest leptons known, could provide an insight to problems such as CP violations, lepton flavour violations, and lepton universality. Moreover, τ -leptons are the only leptons heavy enough to decay via hadronic mode, therefore allowing to study also strong interactions. They also provide the opportunity to study weak currents and their couplings to gauge bosons. While no one doubts that tau leptons were produced at Belle II they have been not observed yet.

Belle II experiment, which is located on SuperKEKB accelerator in Tsukuba, Japan, is a major upgrade of Belle experiment. SuperKEKB is asymmetric electron-positron collider with $\sqrt{s} = 10.58 GeV$ that corresponds to $\Upsilon(4S)$ resonance which in its turn mainly decays into $B \bar{B}$ mesons. It consists of two beam pipes - low energy ring (LER) where 4 GeV positrons run and high energy ring (HER) for 7 GeV electrons (see 1). Because of the energy asymmetry rest frame of B mesons is boosted and proper half time is extended allowing them to travel larger distances. Inasmuch as a lot of B-mesons are produced such experiments are called B-factories. B-factories are precision high energy physics experiments with low particle abundance. This means that they allow to perform measurements in very clean experimental conditions. The cross section of tau-pair creation is comparable to one of B-mesons, so there are also a lot of taus produced. Belle II detector is used to register all collision products at SuperKEKB. It consists of various components designated to specific purposes (see 2). Pixel silicon detectors (PXD) and silicon strip sensors (SVD) are used for decay vertex position measurements; central drift chambers (CDC) are used for measuring trajectories, momenta and dE/dx for charged particles; time of propagation (TOP) counters and ring-imaging Cherenkov counters (A-RICH) for particle identification; electromagnetic calorimeter (ECL) for energy measurements of photons and electrons; iron flux-return outside of the coil to identify muons and K_s^0 mesons. Particle identification detectors are not calibrated yet, though. (Source: [1])

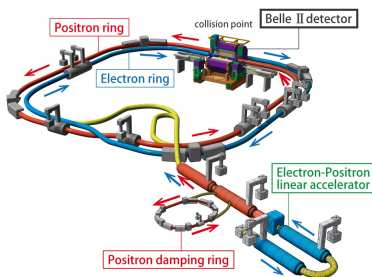


Figure 1: SuperKEKB accelerator

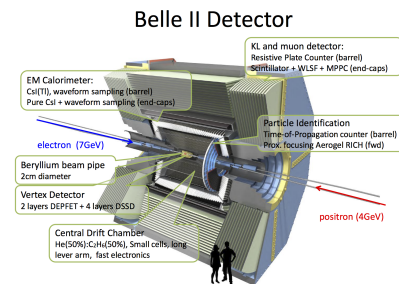


Figure 2: Belle II detector

2 Tau Properties Overview

At Belle II tau leptons are created in e^+e^- collisions (figure 3). The τ -lepton has mass equal to 1,77 GeV which is substantially larger than masses of muons and electrons (105 and 0.5 MeV respectively). Like its lighter counterparts τ has spin 1/2 and its electric charge equals to 1. Life-time of τ particles is $2.9 * 10^{-13}s$ which means that we do not detect taus directly but only its decay products. τ -leptons decay mainly into charged pions, muons or electrons in association with tau-neutrinos. Typical decay branching ratios are listed below (source: PDG).

- Charged pion, neutral pion and tau neutrino - 25.49 %;
- Charged pion and a tau neutrino - 10.83 %;
- Charged pion, two neutral pions, and a tau neutrino - 9.26 %;
- Three charged pions and a tau neutrino - 9.80 %;
- Tau neutrino, electron and electron antineutrino - 17.82 %;
- Tau neutrino, muon and muon antineutrino - 17.39 %;

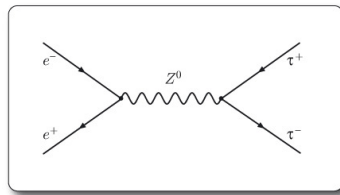


Figure 3: tau production diagram

Because of neutrino presence tau-leptons are difficult to reconstruct. Neutrinos could not be detected hence missing momentum and missing energy are always present in tau reconstruction. Some τ decay diagrams are given in figures 4 and 5.

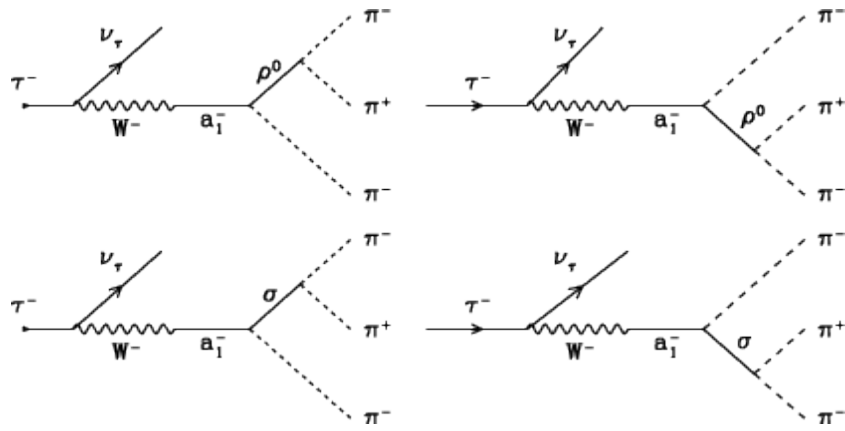


Figure 4: $\tau^- \rightarrow \pi^- \pi^- \pi^+$. Source: [2]

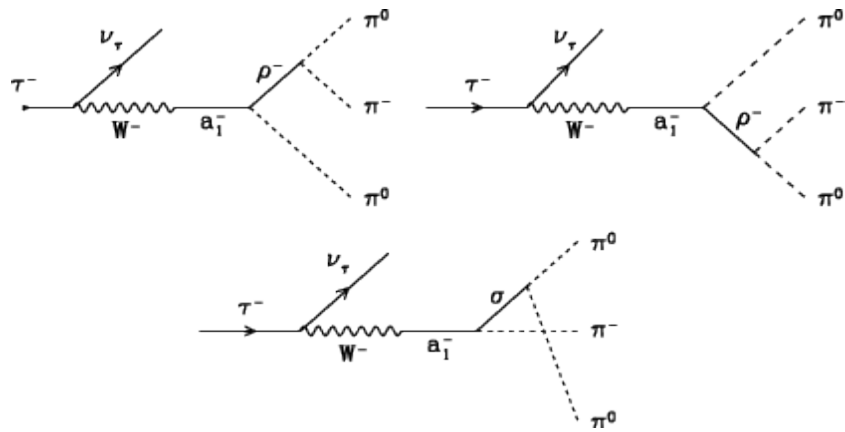


Figure 5: $\tau^- \rightarrow \pi^0 \pi^0 \pi^-$. Source: [2]

3 Event Selection

Processes of $e^+e^- \rightarrow \tau^+\tau^-$ where one τ (signal) goes to 3 hadrons (and neutrino) and another (tag) decays to one hadron or a lepton (with neutrinos) were examined. This type of decay is depicted on Figure 5. Events were reconstructed with a help of basf2 framework which is constructed of C++ modules that are loaded to the path and by python steering script. To select possible candidates for tau decays following criteria were used on each track:

- $p_T > 0.1$ GeV
- $-5 < dz < 5$ [cm]
- $-1 < dr < 1$ [cm]
- $-0.8660 < \cos\theta < 0.9535$

Here: p_T is the transverse momentum of daughter particles (pions); dz and dr - longitudinal and transverse component of particles' tracks with respect to the primary vertex. Photons were selected with following restrictions:

- $E_\gamma > 0.05$ GeV
- $-0.8660 < \cos\theta < 0.9535$

Here $E_\gamma > 0.05$ is the energy of photon and θ is the angle with respect to the beam. There was one additional requirement that there are exactly 4 charged tracks in the event with net charge equal to 0. **It is important to emphasize that particle identification detectors are not calibrated yet, hence we cannot explicitly select events only with hadrons at the final state of signal side.** There are 7 background processes that satisfy all the conditions listed above.

Table 1: Possible background events

$e^+e^- \rightarrow$	σ , nb	Comments	name in scripts
$e^+e^- \gamma$	300 ± 3	photon interacts with detector creating a another pair particles	'ee'
$\mu^+\mu^-\gamma$	1.148 ± 3	similar to the one above	'mumu'
$e^+e^-e^+e^-$	39.7 ± 0.1		'eeee'
$e^+e^-\mu^+\mu^-$	18.9 ± 0.1		'eemumu'
$q_i\bar{q}_i$	1, 61, 0.4, 0.38, 1.3 respectively	$i = u, d, s, c$	'udsc'
$B\bar{B}$	1.05 ± 0.1	$\Upsilon(4S) \rightarrow B\bar{B}$	'mixed', 'charged'

4 Analysis

To distinguish between signal and background events several variables were used based on event kinematics.

Table 2: Variables

Variable	Name of variable in analysis script	Description
$ T $	'thrustValue'	magnitude of thrust value
E_{vis}	'visibleEnergyCMS'	sum of energies of all detected particles of event in cms frame
M_{miss}^2	'missingMass2'	squared missing mass
P_{miss}	'vpho_missingMomentumOfEvent'	magnitude of missing momentum
$E_{\tau,1}$	'vpho_tau0_P4_cms_3'	Energies of signal and
$E_{\tau,2}$	'vpho_tau0_P4_cms_3'	tag taus in cms frame
θ_{miss}	'vpho_missingMomentumOfEvent_theta'	θ -angle of missing momentum

In signal events taus are produced back-to-back in CMS frame unlike the background that comes from $q\bar{q}$ events or B-meson production. To separate signal from these (and not only) types of backgrounds such quantities as thrust value and thrust axis are used. Thrust axis \vec{T} is defined as unit vector along which total projection of all daughter particles is maximal. The thrust value (the magnitude of thrust axis) then follows (1), assuming that there are N particles in the event.

$$|T| = \max \left\{ \frac{\sum_{i=1}^N |\vec{T} \vec{p}_i|}{\sum_{i=1}^N |\vec{p}_i|} \right\} \quad (1)$$

4.1 Distribution Shape Overview

In figures 6 and 7 distributions of visible energy and thrust value in signal and specific backgrounds are shown. There is an obvious difference in shapes that gives a possibility to suppress these backgrounds. Figure 6 indicates that taus decay closer to the thrust axis and daughter particles have relatively small angles of deviation from primary trajectory. While figure 7 clearly shows that there are unreconstructable particles (neutrinos) in the signal event and no such particles in backgrounds. Because of that visible energy is peaking near collision \sqrt{s} for backgrounds and fails to do so for signal events.

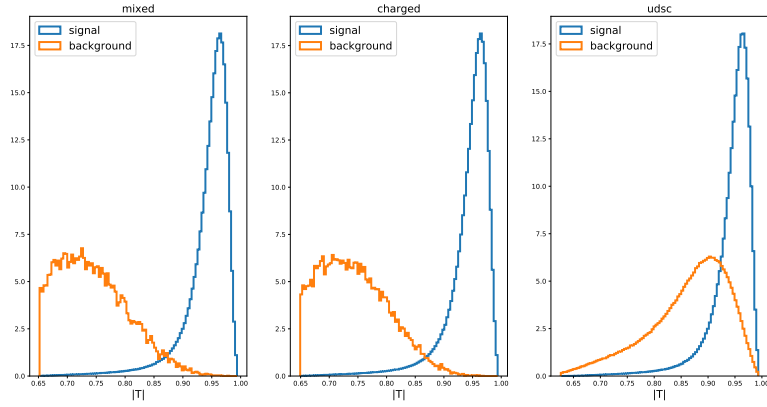


Figure 6: $|T|$ distribution, unity norm.

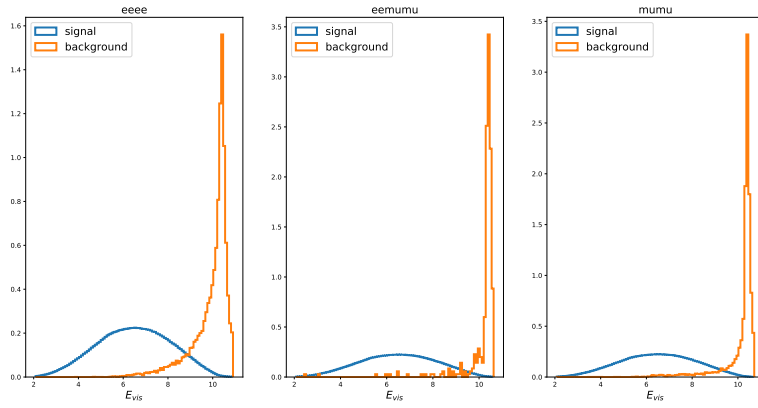


Figure 7: E_{vis} distribution, unity norm.

4.2 Figure of Merit

To define an exact value where one has to put a cut figure of merit (FOM) is used. Figure of merit is defined in a following way:

$$FOM = \frac{S}{\sqrt{S+B}} \quad (2)$$

Here, S is the number of signal events and B is the number of background events. Value that maximizes FOM implies an optimal cut. For every chosen variable FOM was calculated. Signal and backgrounds were weighted accordingly to the luminosity of the sample. Examples are given below. (See Fig 8 and 9) Complete list with FOM-s and signal-background distributions can be found in Section 6. Based on figure of merit, following cuts were defined:

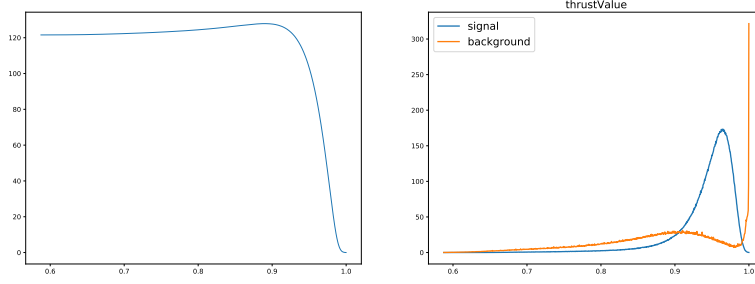


Figure 8: $|T|$ FOM and signal vs. total background distribution

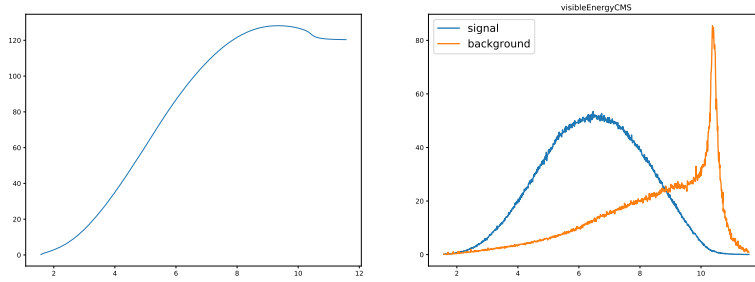


Figure 9: E_{vis} FOM and signal vs. total background distribution

- $|T| > 0.9$
- $E_{\tau,1}, E_{\tau,2} < 5[GeV]$
- $M_{miss}^2 > 0.7[GeV]$
- $P_{miss} > 0.47[GeV]$
- $\theta_{miss} < 2.53$
- $E_{vis} < 9.45[GeV]$

Though, some of them were correlated (i.e. applying them did not change anything sufficiently). Finally, the 3π invariant mass distribution was obtained.

While dominating backgrounds were almost suppressed, the discrepancy between real data and Monte-Carlo simulations was obvious 0.5-0.8 GeV region. One has to mention that background from $e^+e^-\gamma$ process was not considered because of low statistics of simulations. After reevaluating of FOM-s with new simulations (better statistics in $e^+e^-\gamma$ and $\mu^+\mu^-\gamma$ processes) and building new invariant mass distribution a huge peak coming from $e^+e^-\gamma$ in that region was found. The problem was that particle identification detectors are not calibrated yet. If one would consider the quantity E/p where E

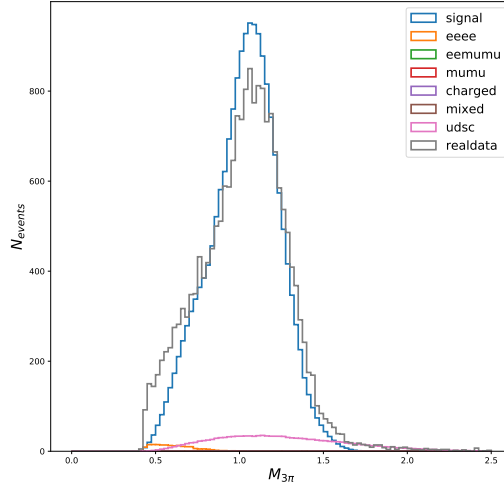


Figure 10: Invariant mass distribution

is energy that was left in calorimeter and p is absolute value of momentum, one would find that for pions $E/p < 1$ and for electrons $E/p \approx 1$.

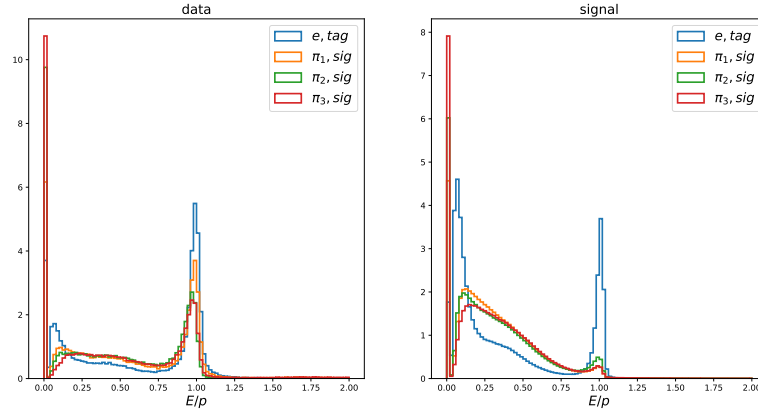


Figure 11: E/p distribution, unity norm

Henceforth, requiring E/p to be smaller than 0.8 for every particle in signal one will cut abundant leptonic background. Additionally, requiring no photons one can reduce the background from $q\bar{q}$ and $e^+e^-(\gamma)$ processes. To summarize, final restrictions are listed below:

- $E/p < 0.8$
- no photons in both sides

- $|T| > 0.9$
- $E_{vis} < 9.7$
- $E_{\tau,1(2)} < 5.14$ (5.16)

5 Conclusions

In this studies tau-leptons were rediscovered at Belle II experiment. With a help of FOM cuts were defined and applied to experimental data from Belle II. With only a couple of restrictions it is possible to suppress almost all dominating backgrounds (see Figure 12) and obtain a clean sample of tau-leptons (Figure 13).

Table 3: Signal contamination

Background	fraction %
$e^+e^-\gamma$	0.9
$\mu^+\mu^-\gamma$	0.03
$e^+e^-e^+e^-$	0.02
$e^+e^-\mu^+\mu^-$	0.02
$q_i\bar{q}_i$	12.5
$B\bar{B}$	0.02

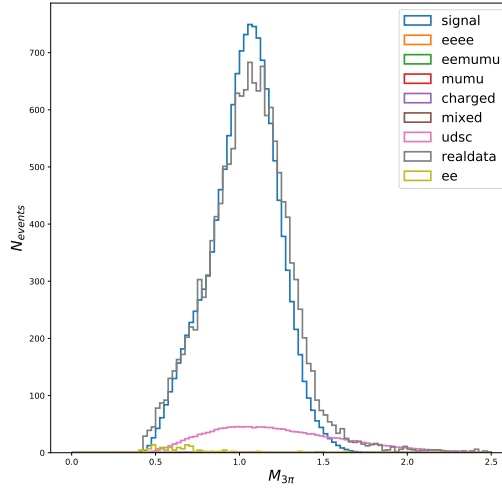


Figure 12: Invariant mass distribution

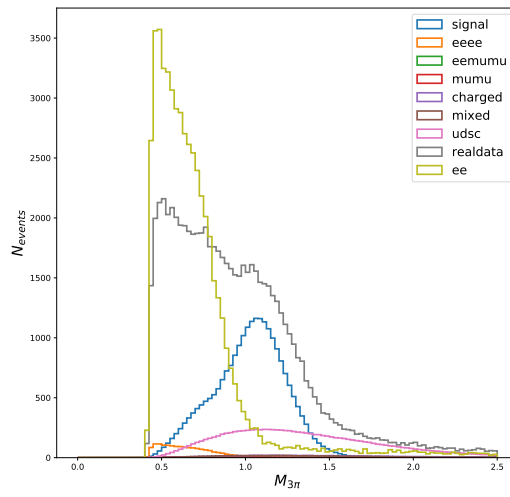


Figure 13: Invariant mass distribution before cuts are applied

6 Appendix

Figures of Merit

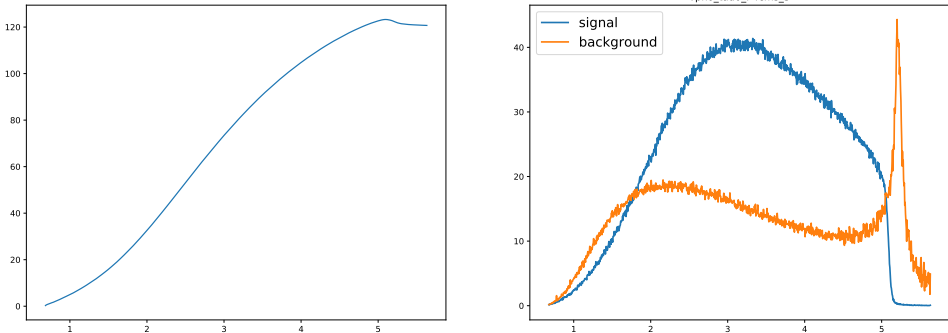


Figure 14: $E_{\tau,1}$ FOM

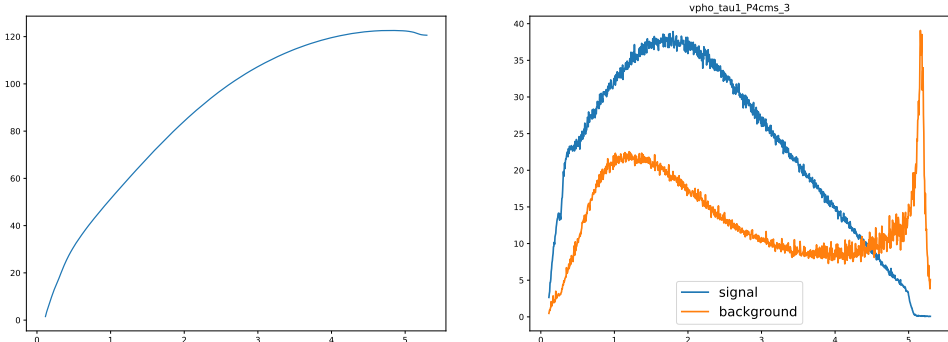


Figure 15: $E_{\tau,2}$ FOM

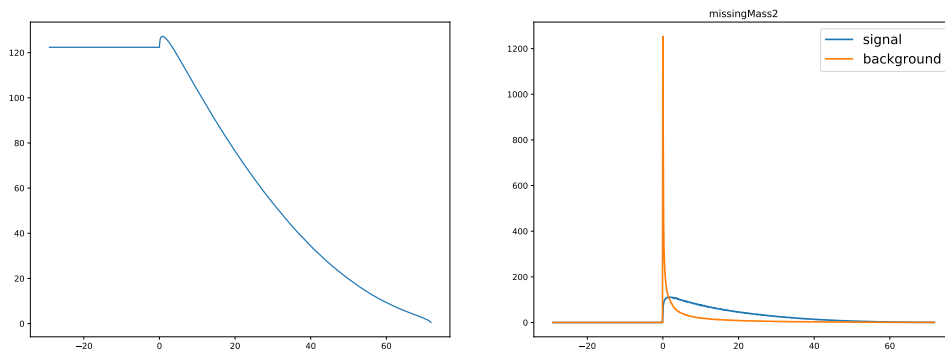


Figure 16: M_{miss}^2 FOM

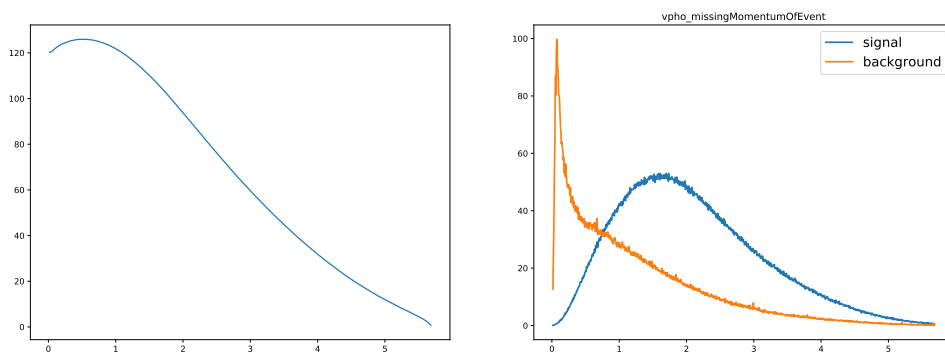


Figure 17: P_{miss} FOM

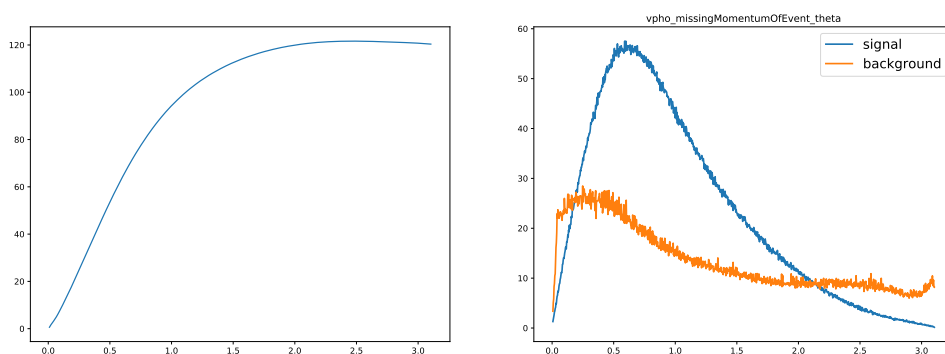


Figure 18: θ_{miss} FOM

Shape Distributions

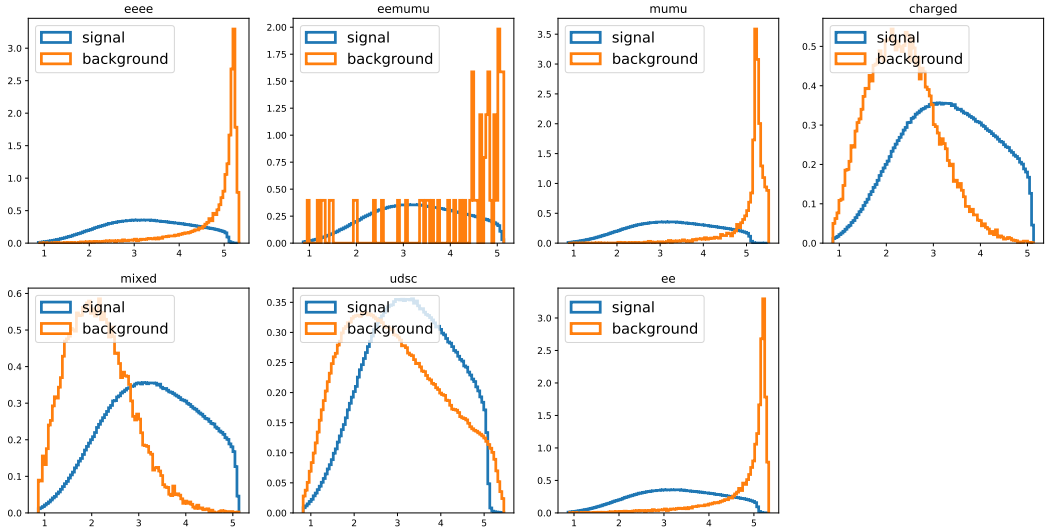


Figure 19: $E_{\tau,1}$ unity norm

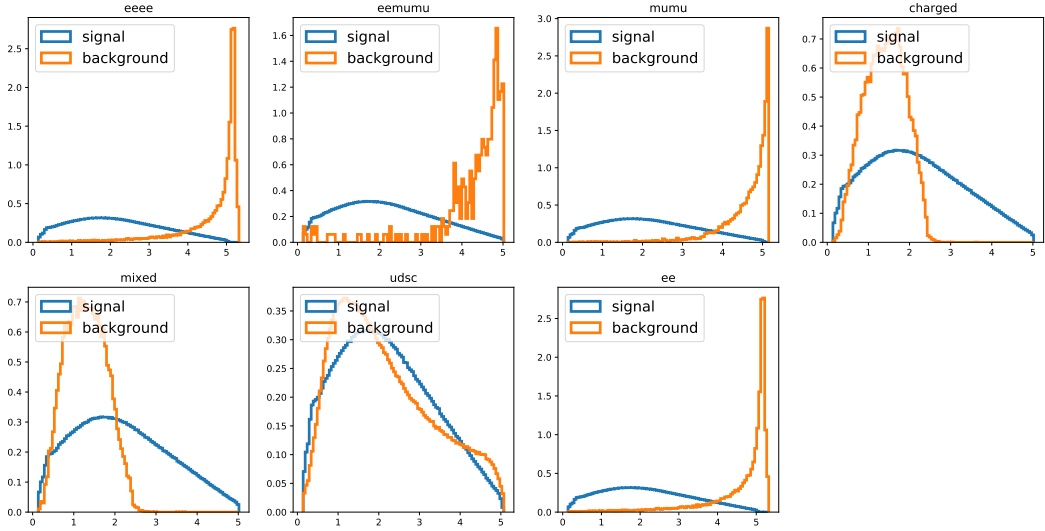


Figure 20: $E_{\tau,2}$ unity norm

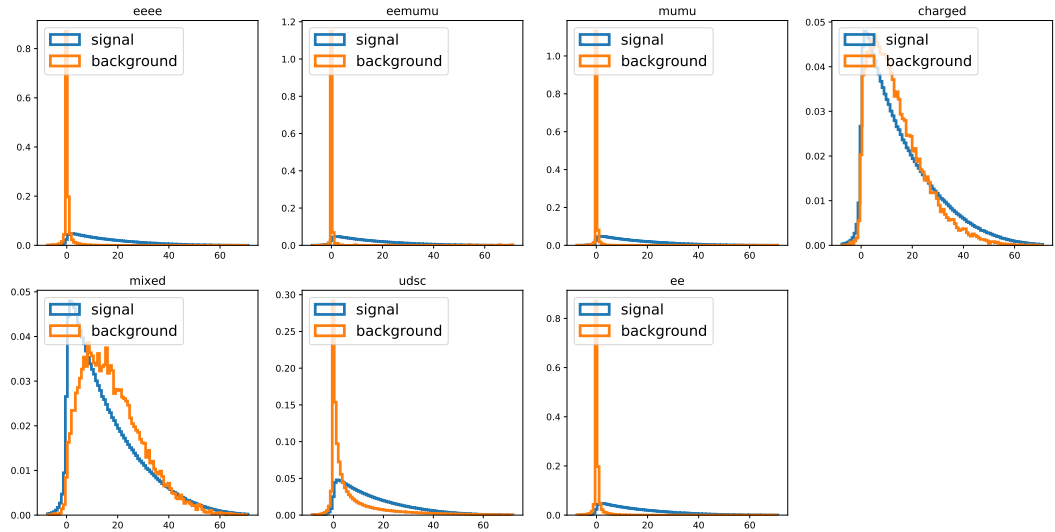


Figure 21: M_{miss}^2 unity norm

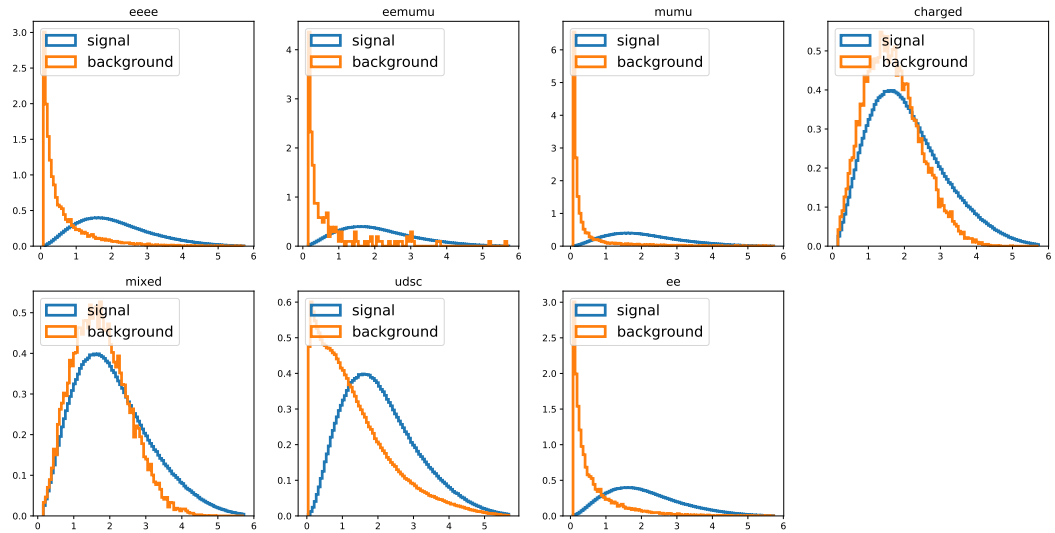


Figure 22: P_{miss} unity norm

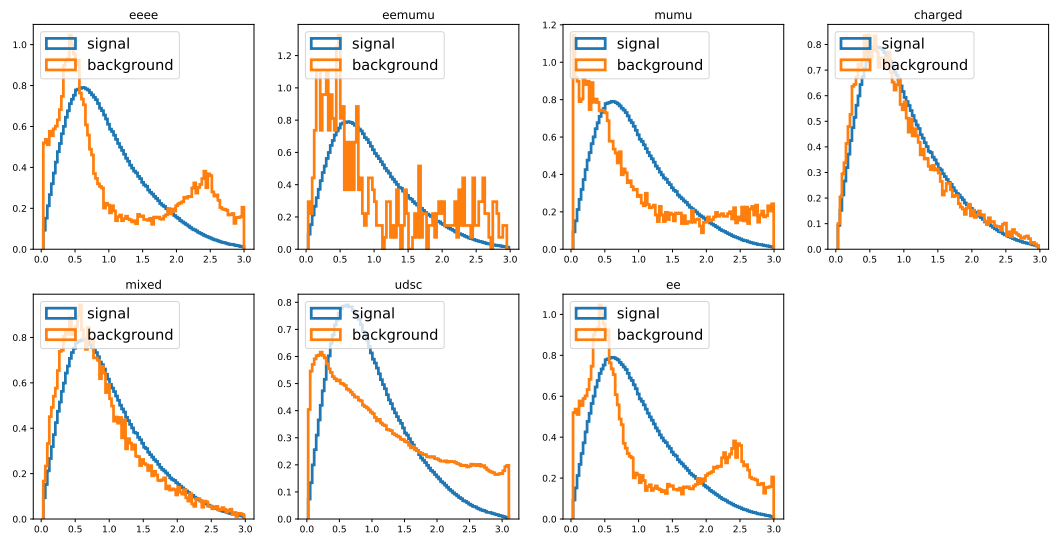


Figure 23: θ_{miss} unity norm

References

- [1] Belle II collaboration
- [2] Three-pion decays of the tau lepton, the $a_1(1260)$ properties, and the $a_1\rho\pi$ Lagrangian *Vojik, Lichard; arXiv:1006.2919*